#### ORIGINAL RESEARCH ARTICLE



# Examining subsurface response to an extreme precipitation event using HYDRUS-1D

Claudia R. Corona D | Shemin Ge

Geological Sciences, Univ. of Colorado, Boulder, CO 80309, USA

#### Correspondence

Claudia R. Corona, Geological Sciences, Univ. of Colorado, Boulder, CO 80309, USA.

Email: claudia.corona@colorado.edu

Assigned to Associate Editor Asim Biswas.

#### **Funding information**

National Science Foundation (NSF), Division of Earth Sciences, Grant/Award Number: #EAR-1834290

#### Abstract

North-central Colorado experienced an extreme precipitation event (EPE) in September 2013, during which the equivalent of 80% of the region's annual average precipitation fell in a few days. Widespread flooding occurred above ground, but the shortand long-term subsurface response remains unclear. The objective of the study is to better understand the dynamic subsurface response, namely how the water table and soil water storage responded to a large amount of infiltration in a short period of time and how the hydrologic properties of the subsurface influence the response. Better understanding of subsurface response to EPEs is expected to increase with the advent of more intense and frequent EPEs in the coming decades. A one-dimensional subsurface flow model using HYDRUS-1D, was built to simulate and examine infiltration of an EPE at a site in the Boulder Creek Watershed, Colorado. Model calibration was conducted with local field data to fit site observations over a 6-yr period. A rapid water table depth response in field observations was observed, with the modeled subsurface storing water for 18 mo acting as a hydro-buffer during recovery. To examine influence on model results, a sensitivity study of soil hydraulic parameters was conducted. The sensitivity study found that changes in n, an empirical parameter related to pore-size distribution, most significantly affects water table depth. The implications are that one-dimensional models may provide useful estimates of water table fluctuations and subsurface hydro-buffer capacities in response to EPEs, which could be of use to regions preparing for EPE effect on water resources.

# 1 | INTRODUCTION

At the extremes of precipitation occurrence are the events that result in floods or droughts, known as extreme precipitation events (EPEs). On the wetter side, EPEs are defined by greater-than-average precipitation events that can span minutes to days (Lehmann et al., 2015; Trenberth et al.,

**Abbreviations:** 1D, one-dimensional; BcCZO, Boulder Creek Critical Zone Observatory; EPE, extreme precipitation event; WY, water year.

2003; Westra et al., 2013). An EPE occurred in September 2013 along the Colorado Front Range, United States, which unleashed 430 mm of rain (84% of the 510 mm annual average for the region) in a few days (Uccellini, 2014). A 100-km corridor between Fort Collins, CO, and Aurora, CO, experienced the most intense precipitation, which led to a disaster zone declaration by the Federal Emergency Management Agency for a ~65,000-km² area, which is about a quarter of the state (Uccellini, 2014). The resulting floods ravaged foothill and valley communities, causing billions of

This is an open access article under the terms of the Creative Commons Attribution License, which permits use, distribution and reproduction in any medium, provided the original work is properly cited.

© 2022 The Authors. Vadose Zone Journal published by Wiley Periodicals LLC on behalf of Soil Science Society of America

Vadose Zone J. 2022;e20189.

dollars of property and infrastructure damage and the tragic loss of eight lives (Coffman, 2013). The above-surface flooding response to similar extreme events has been documented and photographed in Colorado for over 125 yr (BASIN, 2005). However, the subsurface physical response to EPEs is not as easily observed or measured in real-time, making it one of the more poorly understood hydrogeologic topics of the 21st century (Vereecken et al., 2015).

Subsurface response to EPEs may involve rapid fluctuations of soil water storage and abrupt water table depth changes (Freeze & Witherspoon, 1967; Jasechko & Taylor, 2015; Tashie et al., 2016). French et al. (1996) examined subsurface response to regular and intense precipitation at a highelevation study site in the southwest region of the United States. The shallow soils at this high-elevation site extended 1 m below ground level to fractured bedrock. The hypothesis stated that if infiltrating water could penetrate this 1-m physical transition, then it could likely result in groundwater recharge (French et al., 1996). Examination of soil water data found that fall and winter events (October-April) more often infiltrated below a 1-m depth. It was suggested that this was due to (a) the longer duration of the precipitation events and snowmelt and (b) lower evapotranspiration rates. In contrast, summer events (May-August) were observed to be of short duration and affected by high evapotranspiration, diminishing infiltration past the 1-m depth. The study concluded that it was unclear how soil profiles deeper than 1 m may respond to varying precipitation events, either normal or intense, and more research was suggested.

Ng et al. (2010) studied the effects of different climate predictions on diffuse episodic recharge for a study site in the southern High Plains of the United States. They found that high-rainfall periods, equivalent to EPEs, were more likely to result in recharge during the winter months (December–March), when evapotranspiration is lower and plant roots are dormant. At the same time, the study acknowledged that EPEs and interannual variability were not represented, which may have underestimated a significant fraction of the total recharge predicted. They called for future studies to use field measurements of interannual variability, including EPEs, where possible, especially for predicting recharge in arid environments, as is the case for the southwestern United States, the Middle East, most of Australia, and northern African.

Shao et al. (2018) found that consecutive wet years promoted groundwater recharge more significantly than years with average precipitation. This is an important finding because the numbers of wetter years and drier years are expected to increase in the future, while years of average precipitation are expected to decrease (Lehmann et al., 2015; Trenberth, 2011; Wasko et al., 2016). In particular, precipitation events are expected to shorten in duration and increase in intensity (Pendergrass & Knutti, 2018; Pfahl et al., 2017; Prein et al., 2017). This highlights an urgent need to move

#### **Core Ideas**

- Effects of extreme precipitation events on subsurface processes were explored through modeling.
- A model was built to fit field data and simulate varying water table depth over a 6-yr period.
- The modeled subsurface stores water for 18 mo, acting as a hydro-buffer during recovery.
- Model results are most sensitive to *n*, an empirical value related to pore-size distribution.

beyond annual precipitation and use comprehensive interannual variability, including EPEs, in modeling efforts to better understand subsurface response.

A better understanding of subsurface response to EPEs can improve future planning of groundwater resource allocations (Gurdak et al., 2009; Kløve et al., 2013). Using the HYDRUS-1D subsurface flow model with average soil hydraulic parameters estimated by Schaap et al. (2001), Corona et al. (2018) found that the prescribed flux (precipitation) and period (30, 180, 365, and 730 d) were the most statistically significant predictors of whether an infiltration flux became steady or transient recharge. The study examined the combinations of daily precipitation rates and soil types that could lead to recharge, finding that daily precipitation of lower intensity and finer-grained soils resulted in little to no recharge, whereas daily precipitation of greater intensity and coarser-grained soils, like sand, resulted in greater recharge. A sensitivity study of parameter influence on infiltration fluxes in the vadose zone was also conducted but did not consider precipitation variability within a period and the subsequent soil response. Where available, field observations of water table depths and soil water content changes are a useful guide to better understand the EPE-subsurface connection (Jasechko & Taylor, 2015; Thomas et al., 2016). Where data are limited, numerical models coupled with available field data can provide some understanding of the EPEsubsurface connection (Dadgar et al., 2020; Mo'allim et al., 2018).

The objective of this study was to build a HYDRUS-1D model with local field data and examine how the subsurface responded to the EPE that affected north-central Colorado in September 2013. This study addressed the following questions: How does the water table fluctuate in response to the EPE? What can a sensitivity study show about parameter uncertainty? How does soil water storage respond to the EPE?

Exploring these questions can shed new light on infiltration flux through the subsurface, dynamic changes in subsurface water storage, and the temporal extent of subsurface system response to EPEs.

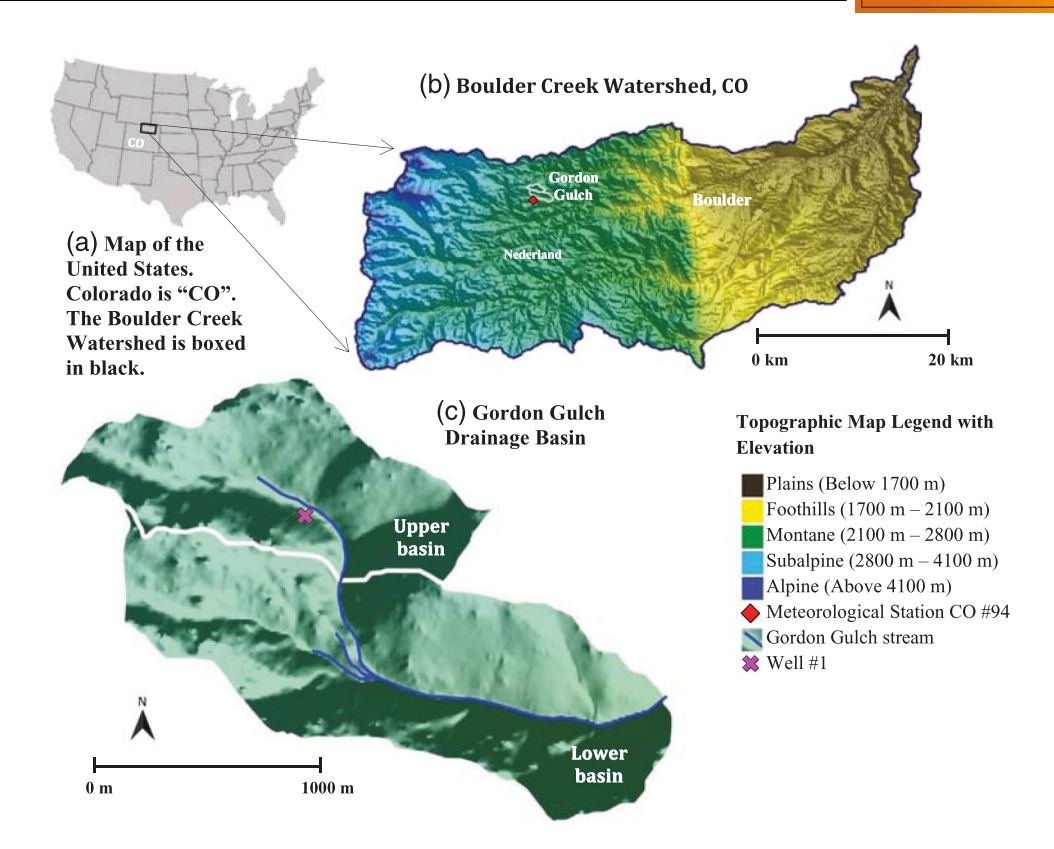


FIGURE 1 (a) Map of the United States with the Boulder Creek Watershed, CO, boxed in black. (b) Topographic map with elevation of the Boulder Creek Watershed. The Gordon Gulch drainage basin is outlined in white. (c) Topographic map of the Gordon Gulch drainage basin, which is in the Montane zone of ~2,400–2,800 m. The blue line indicates a stream. The pink "X" marks the location of Well 1, which is a well in the upper basin that has recorded water table depth at the since December 2011

#### 2 | MATERIALS AND METHODS

# 2.1 | Study area and field data

The Gordon Gulch drainage basin is located 30 km west of Boulder, CO (2,400–2,800 m asl) (Figure 1). The basin has a total area of ~3.6 km²; the upper basin has an area of ~1.0 km², and the lower basin has an area of ~2.6 km². Gordon Gulch lies in a montane climate zone, with an average annual precipitation of 520 mm yr<sup>-1</sup> (BcCZO, 2020). The basin, hereinafter "Gordon Gulch," was chosen due to the extensive data available. In 2011, the Boulder Creek Critical Zone Observatory (BcCZO) installed six wells in the upper basin of Gordon Gulch. The wells have been monitored and maintained by the BcCZO since December 2011.

Wells 1, 2, and 6 have working pressure transducers that record water table depth variations at 10-min intervals. Well 1 was chosen because it has the largest vadose zone extent (~10 m) of the three wells measuring water table depth, making it the ideal candidate for examining pressure head and soil moisture response to EPEs above the water table. Well 1 is at a horizontal distance of 150 m away from the small ephemeral stream and 12 m higher in elevation above the streambed.

The flow record of the nearest stream gauge has not shown evidence of stream influence on Well 1 (Anderson & Ragar, 2021a; Henning, 2016; Salberg, 2021). In contrast to Well 1, Well 2 is influenced by nearby streamflow, whereas Well 6 is affected by lateral flow and upslope infiltration (Anderson & Ragar, 2021b; Henning, 2016; Salberg, 2021). Wells 2 and 6 are henceforth omitted. Well 1 is screened from a depth of 9.4 m to the bottom of the well at 18.55 m, with an average water table depth of ~9.6 m. The soil lithology of Well 1 is considered representative of the subsurface of the study site based on the geophysical surveys conducted by Befus et al. (2011). For this study, the depth of the well penetrating 10 m of the unsaturated zone and 10 m of saturated zone makes it a good candidate for studying the dynamics of water table fluctuation.

The daily precipitation data are derived from a meteorological station ~3 km south of the well site, at the Sugarloaf Station CO94, managed by the National Atmospheric Deposition Program (NADP, 2020). Although not co-located, the station experienced the same amount of precipitation as the well site (Uccellini, 2014). It has a record of daily precipitation from 1986 to 2017 (NADP, 2020). To align with the available daily precipitation record, only December 2011–December 2017 water table depth data are used in this study.

#### 2.2 Unsaturated flow in the vadose zone

Subsurface processes are difficult to observe and quantify in real-time. Numerical models, such as the public domain HYDRUS source code (Šimůnek et al., 2008), solve Richards' equation to examine one-dimensional (1D) water flow in an unsaturated-saturated porous medium and calculate the overall water mass balance. Ignoring the air-phase flow and thermal effects, Richards' equation has the following form (Richards, 1931):

$$\frac{\partial \theta}{\partial t} = \frac{\partial}{\partial z} \left[ K \left( \frac{\partial \psi}{\partial z} + 1 \right) \right] \tag{1}$$

where  $\theta$  is the water content, t is time (T),  $\psi$  is the pressure head (L),  $K = K(\psi)$  is the unsaturated hydraulic conductivity dependent on the pressure head (LT<sup>-1</sup>), and z is the downward distance from the ground surface (L). HYDRUS-1D implements the van Genuchten (1980) equations that use Mualem's (1976) pore-size distribution model. The van Genuchten (1980) equations are a set of closed-form analytical expressions that provide continuous functional relationships for the soil water retention,  $\theta(\psi)$ , and the unsaturated hydraulic conductivity,  $K(\psi)$ , of a soil:

$$\theta(\psi) = \begin{cases} \theta_{r} + \frac{\theta_{s} - \theta_{r}}{[1 + |\alpha\psi|^{n}]^{m}} & \psi < 0 \\ \theta_{s} & \psi \ge 0 \end{cases}$$
 (2)

$$K = K(\psi) = K_{\rm s} S_{\rm e}^l \left[ 1 - \left( 1 - S_{\rm e}^{\frac{1}{m}} \right)^m \right]^2$$
 (3)

$$m = 1 - \frac{1}{n}, \quad n > 1 \tag{4}$$

where  $S_{\rm e}$  is the effective saturation:

$$S_{\rm e} = \frac{\theta - \theta_{\rm r}}{\theta_{\rm s} - \theta_{\rm r}} \tag{5}$$

where  $\theta_{\rm r}$  and  $\theta_{\rm s}$  denote the residual and saturated water content, respectively;  $K_{\rm s}$  is the saturated hydraulic conductivity;  $\alpha$  is a parameter inversely related to the air-entry pressure; n is the pore-size distribution; and l is a pore-connectivity parameter (van Genuchten, 1980; Mualem, 1976).

Initially, HYDRUS-1D solves equation 1 for  $\psi(z)$ . The unsaturated hydraulic conductivity as a function of pressure head,  $K(\psi)$  in Equation 1, is obtained from Equations 2–5. During each time step,  $K(\psi)$  and  $\theta(\psi)$  values are obtained iteratively, where  $\psi(z)$  values from the prior time step and specified soil parameters  $(K_s, \theta_r, \theta_s, \alpha, n, m, l)$  in Equations 2–5 are used to compute  $K(\psi)$  at every depth and then used

to solve Equation 1 for  $\psi(z)$ . Once the  $\psi(z)$  values between iterations converge, HYDRUS-1D proceeds to the next time step.

# 2.3 | Model setup

The HYDRUS-1D model can be used to analyze water movement in partially saturated and fully saturated porous media (Šimůnek et al., 2013). The model domain is a 1D vertical column extending downward from the land surface to a depth of 50 m. In the model domain, the pressure heads change from negative in the unsaturated zone to positive in the saturated zone. The water table position is found where the pressure head is zero. To reflect the depth of the average water table at the site (Salberg, 2021), the modeled water table was initialized at a 10-m depth.

An initial sensitivity study (not shown) was conducted to identify whether a varying soil column length (z=20, 50, or 100 m) affected water table fluctuations. Model runs showed that the water table fluctuations (where  $\psi=0$  at z=10 m) were very similar when comparing the 50- and 100-m lengths; as a result, a 50-m length was chosen. The soil column is discretized into 241 nodes. A sensitivity study of refining soil profile discretization (101, 201, 241, 301, and 501 nodes) found no significant differences in model results with profile discretization of finer than 241 nodes. The area of interest in this study is the unsaturated zone (z=0-10 m), with denser node spacing in the first 10 m of the profile (z=0-10 m), with a spacing of 0.072 m between nodes. From z=10 to 50 m, node spacing is less dense and increases linearly from 0.072 to 0.72 m.

A prescribed flux is applied as the top boundary condition (Figure 2). A deep drainage flux is applied at the bottom of the soil column. The drainage flux out of the column,  $q(\psi)$ , is approximated by the following expression (Hopmans & Stricker, 1989):

$$q(\psi) = -Ae^{(B|\psi_{\text{bottom}} - \text{GWL}|)}$$
 (6)

The variable  $q(\psi)$  (LT<sup>-1</sup>) is the flux across the bottom boundary, and A (LT<sup>-1</sup>) and B (L<sup>-1</sup>) are adjustable empirical parameters. The  $\psi_{\text{bottom}}$  (L) is the pressure head at the bottom boundary, and GWL (L) is a long-term equilibrium water table position relative to the bottom boundary, where GWL = 50 m for this study. We calibrated the A and B parameters iteratively to fit the available water table data following the methodology of Neto et al. (2016). In this study, the unit of length (L) is meters (m), and the unit of time (T) is days (d). Model setup allows for a conceptualization of the system such that model results can explain the field observations.

The lithology is characterized by four soil types: soil, saprolite, weathered bedrock, and unweathered bedrock (Figure 2).

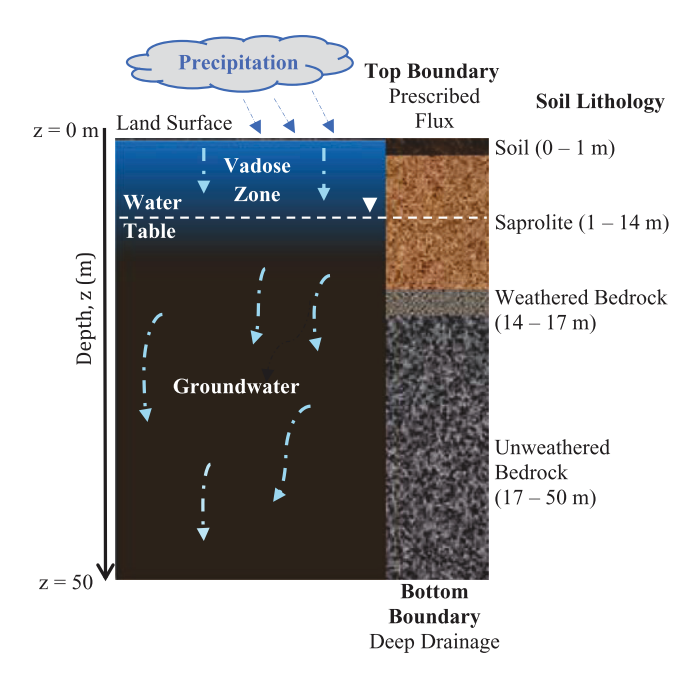


**FIGURE 2** One-dimensional model setup. The top boundary is defined by a prescribed flux condition. The bottom boundary is defined by a deep drainage condition. The soil lithology is characterized by the following thickness: 1 m soil, 13 m saprolite, 3 m weathered bedrock, and 33 m unweathered bedrock

This composition has been identified by geophysical surveys, soil pit hand-dug records, and well lithology records (Anderson et al., 2013; Befus et al., 2011; Shea, 2013). The initial parameters,  $K_s$ ,  $\theta_r$ ,  $\theta_s$ ,  $\alpha$ , n, (Table 1), are obtained from a previous calibrated model and field study of the upper Gordon Gulch drainage basin (Henning, 2016). Figure 2 shows the soil stratigraphy of the well, where a portion of the saprolite layer (10-14 m), the entire weathered bedrock layer (14– 7 m), and the entire unweathered bedrock layer (17-50 m) are below the 10-m water table and considered fully saturated. Because there is no pore space for air to enter in the saturated zone, changes to the  $\alpha$  value for the unweathered and weathered bedrock layers have little influence on model results. Similarly, adjusting the n value for the fully saturated layers would not influence model results.

During initial calibration, the tortuosity parameter l was calibrated in conjunction with the other parameters. A literature review found that a tortuosity value of l = 0.5 led to poor predictions of unsaturated hydraulic conductivity in 235 soil samples of varying textures (Schaap & Leij, 2000). Schaap and Leij (2000) suggested that the tortuosity be optimized at values of -1 or lower. Yates et al. (1992) suggested that optimal values for l can range from -3 to >100. Thus, simulations were run with the initial value of 0.5 and in increments/decrements of 0.5 from -10 to 10. A tortuosity of l = -2 was determined to be the optimal value for this study.

The model is initialized with a prescribed pressure head distribution that linearly decreases from  $\psi = -10$  m at the surface (z = 0 m) to  $\psi = 40 \text{ m}$  at the bottom of column (z = 50 m). For model spin-up we use the daily average precipitation minus evapotranspiration as the recharge boundary condition on the model top. To account for evapotranspiration, we examined previous studies that estimated potential evapotranspiration for the Gordon Gulch basin and found that potential evapotranspiration values may range from 31 to >100% of the annual average precipitation (Hale, 2022; Langston et al., 2015; Salberg, 2021). Most recently, Salberg (2021) calculated monthly total evapotranspiration loss for a catchmentscale water budget of Gordon Gulch. They suggested that ~435 mm of the average 580 mm annual precipitation of the Gordon Gulch drainage basin was lost to evapotranspiration, a  $\sim$ 75% average. Thus, an evapotranspiration rate of 75% is used, which is also backed by regional climate model estimates of evapotranspiration (55-85%) (Sanford & Selnick, 2013: Reitz et al., 2017). Given the 75% loss to evapotranspiration, the model recharge is 25% of the precipitation amount.

The model was spun-up for 400 d to allow the model to equilibrate to a steady state, considering the initial condition. The initial condition is the state from which the model's transient simulations can initiate. For the transient simulations, we apply the 2011–2017 precipitation record minus evapotranspiration. The transient model is run and calibrated by iteratively adjusting the soil hydraulic parameters  $K_s$ ,  $\theta_r$ ,  $\theta_s$ ,  $\alpha$ , and n. Calibration results in a parameter scenario that allows the modeled water table to best match the field observations. We note that though these parameters may not be the only ground truth parameter scenario in the field, they represent the best

TABLE 1 van Genuchten parameters used to define the four soil layers for the base case

Soil layer	Residual water content	Saturated water content	Parameter inversely related to air-entry pressure m <sup>-1</sup>	Pore-size distribution	Saturated hydraulic conductivity m d <sup>-1</sup>	Tortuosity
Soil	0.10	0.28	0.18	1.50	3.0	-2
Saprolite	0.10	0.20			2.0	
Weathered bedrock	0.05	0.15			1.5	
Unweathered bedrock	0.05	0.10			1.0	

scenario based on available data and provide model output that can most closely match the field observations.

# 2.4 | Statistical indicators

The  $R^2$  and the RMSE are used in this study to provide a first-order assessment comparing the modeled and observed water table fluctuations. The  $R^2$  describes the proportion of the variance of the field observation data that can be explained by the model. The  $R^2$  can range from 0 to 1, with higher values indicating less probability of error variance;  $R^2$  values >.50 are acceptable (Moriasi et al., 2007).

The RMSE index quantifies the error of a model in predicting observations by measuring the residual spread from the observations. In Equation 7,  $P_i$  denotes the model predicted values, and  $O_i$  denotes the field observations for a sample n.

RMSE = 
$$\sqrt{\frac{\sum_{i=1}^{n} (P_i - O_i)^2}{n}}$$
 (7)

The RMSE is the square root of the average of the squared errors. Thus, a lower RMSE typically suggests a lower chance of error, with an RMSE of zero suggesting a perfect fit between the predicted and observed. The RMSE is commonly used because it calculates the error of a comparison in the units of the constituent of interest (Moriasi et al., 2007; Reusser et al., 2009). It has been proposed that RMSE values less than half of the standard deviation of the observations may indicate a low probability of error (Moriasi et al., 2007; Singh et al., 2005).

# 2.5 | Sensitivity analysis

Once the base case is constructed, we conduct (a) a sensitivity study of parameters to understand parameter influence on results and (b) post-processing analysis of simulated soil water storage. The sensitivity study focuses on the local unsaturated zone, where we consider only the soil (0–1 m) and the saprolite (1–14 m) layers. Six sensitivity simulations are conducted for three parameters (two per parameter): the residual water content  $(\theta_r)$ , the empirical parameter inversely related to the air-entry pressure  $(\alpha)$ , and the pore-size distribution (n). For each sensitivity simulation, the respective parameter is increased or decreased for the soil and saprolite layers of the base case model (Table 2). The chosen range of values reflects low and high averages across the 12 soil textural classes predicted by the ROSETTA Soil Catalog (Schaap et al., 2001). For  $\theta_r$ , a decrease from the base case ( $\theta_r = 0.01$ ) suggests less water remaining in a soil pore at high tension. An increase  $(\theta_r = 0.15)$  suggests more water remaining in a soil pore at high tension, which may be indicative of a clay-rich soil (van

**TABLE 2** Sensitivity analysis changes to van Genuchten parameters

Soil layer	Residual water content	Parameter inversely related to the air-entry pressure	Pore-size distribution			
		$\mathrm{m}^{-1}$				
Base case	0.10	0.18	1.50			
Increase from the base case						
Saprolite	0.15	2.00	5.50			
	0.15	2.00	5.50			
Decrease from the base case						
Saprolite	0.01	0.10	1.25			
	0.01	0.10	1.25			

Genuchten, 1980). For  $\alpha$ , a decrease ( $\alpha = 0.10$ ) suggests a higher minimum matric suction required for air to enter pore spaces, whereas an increase ( $\alpha = 2.00$ ) suggests a lower minimum matric suction required. For n, a decrease (n = 1.25) represents a wider pore-size distribution (larger variation in pore sizes in the soil), whereas an increase (n = 5.50) represents a narrower pore-size distribution.

A preliminary sensitivity analysis of changes in the saturated water content  $(\theta_s)$  showed similar trends in water table fluctuations to changes in residual water content  $(\theta_r)$ . The residual water content is often overlooked and difficult to assess, in contrast to  $\theta_s$ , which is often easier to characterize (van Genuchten, 1980; Vanapalli et al., 1998). In a landmark paper, van Genuchten (1980) suggested that the poor matching between the predictive soil water retention curve and the observed curve could be attributed to the  $\theta_r$  value, which was estimated to be zero. van Genuchten (1980) suggested that future studies consider the importance of having an independent procedure for estimating  $\theta_r$ . Despite decades of progress, correctly assessing the  $\theta_r$  for a soil remains a challenge (Nimmo, 2006; Vanapalli et al., 1998; Vogel et al., 2001). Including it in the sensitivity analysis as in the present study could help us better understand the consequences of changing the residual water content in subsurface flow modeling. Changes to the saturated hydraulic conductivity,  $K_s$ , and tortuosity, l, had little effect on model results and are henceforth omitted.

## 3 | RESULTS

#### 3.1 | Base case

Water table depths of the field observations and the base case model are compared in Figure 3a. Actual model recharge (m d<sup>-1</sup>), described as 25% of the actual precipitation record, is plotted on the second y-axis. Throughout the 6-yr period, field

CORONA AND GE Vadose Zone Journal 250 7 of 15

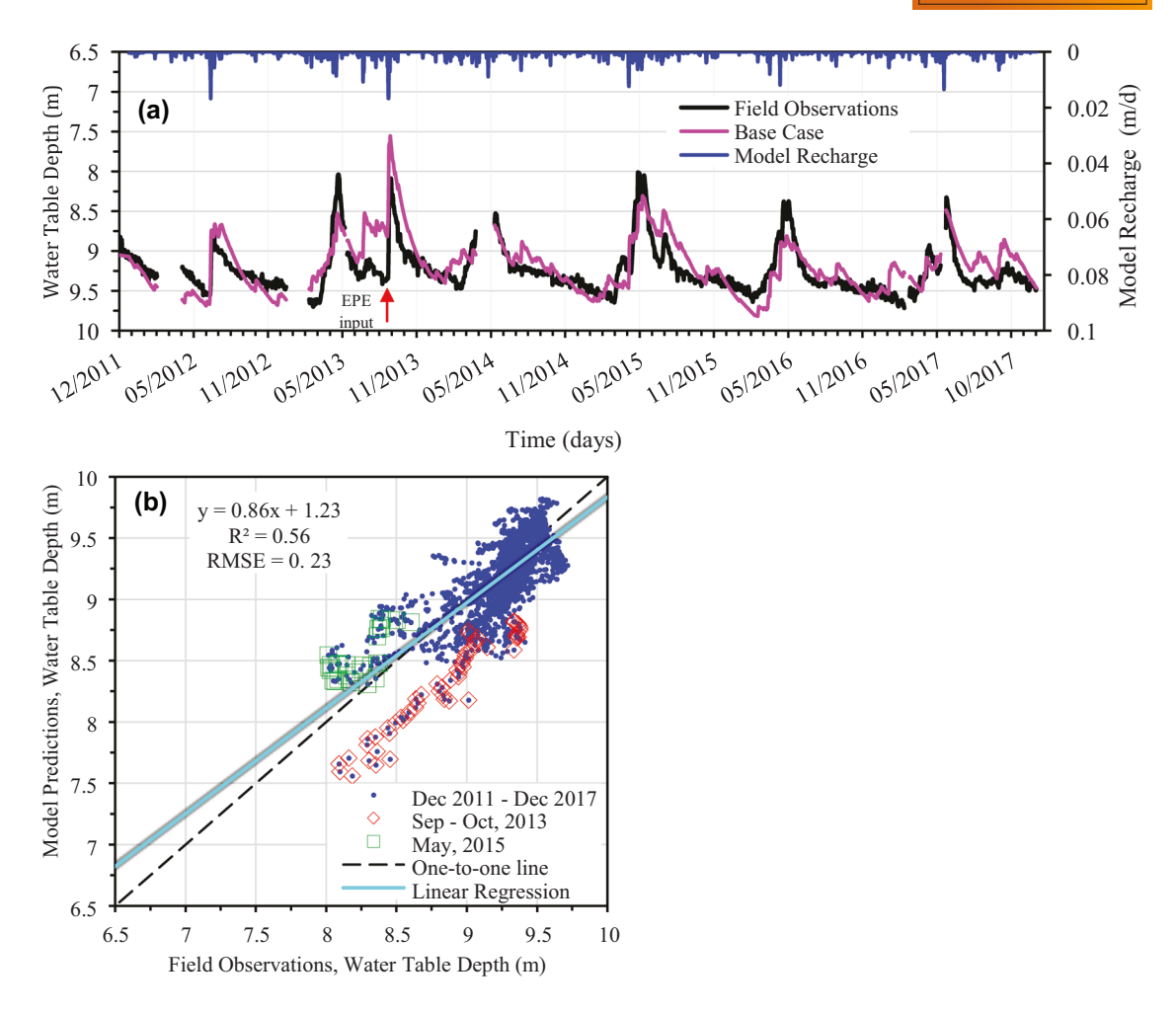


**FIGURE 3** (a) Time series of field observations and base case model predicted water table depths (m). (b) Linear regression of the model predictions versus the field observations. The  $R^2$  value is a statistical measure of how close the data plotted are to the fitted regression line (light blue). The RMSE evaluates how well the model fits the field observations

observations of water table depth range from  $\sim$ 8.0 to  $\sim$ 9.7 m. Similarly, base case water table depths range from  $\sim$ 7.6 to  $\sim$ 9.8 m. Visually, the base case matches the field observations well.

The September 2013 EPE (Figure 3a, red arrow) is an exception, where the base case model predicts a shallower water table depth than the field observations. A linear regression between the model predictions and the field observations suggest that the model predicts shallower water table depths relative to the field observations (Figure 3b). For example, during the EPE, an  $\sim$ 8.1-m field measurement was predicted to be  $\sim$ 7.6 m by the base case. Although the model overestimates water table depths at certain times during the EPE, the changes remain within  $\sim$ 6% of the field observations, suggesting an overall good fit.

The green squares indicate a rainy May in 2015, and the base case model predicts deeper water table depths compared with the field observations. Around May 2015 (Figure 3a), the base case predicts a water table depth of  $\sim$ 8.3 m, compared with the shallower depth of  $\sim$ 8.0 m of the field observations.

This underestimation is within 4% of the field observation. The linear regression gives a  $R^2$  value of .56 for the 6-yr time series.

Singh et al. (2005) published guidelines stating that RMSE values less than half the standard deviation of the field observation data could be interpreted as indicating a good fit of the model to the field observations. The standard deviation of the field observations for the 6-yr period is 0.40 m. Following the guidelines of Singh et al. (2005), an RMSE value ≤0.20 m is considered a good model fit. For this study, RMSE values between 0.20 and 0.30 m indicate an acceptable model fit. Models with an RMSE >0.30 m indicate a poor fit. The base case RMSE (0.23 m) indicates an acceptable model fit.

# 3.2 | Sensitivity analysis of hydraulic parameters

With the base case established, we examine parameter uncertainty in model results by conducting a sensitivity analysis of

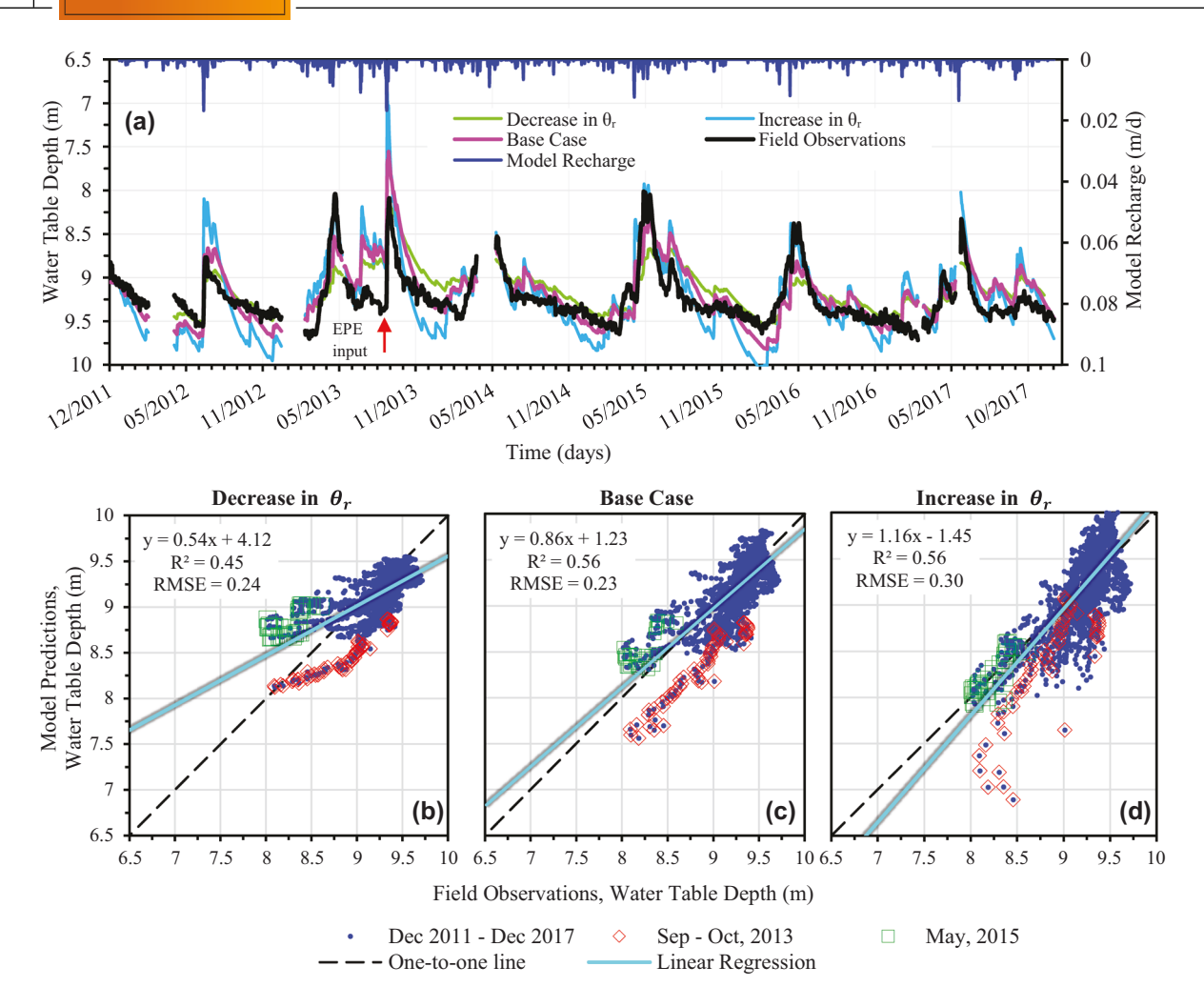


**FIGURE 4** (a) Time series of field observations and model predictions of water table depths for varying residual water content,  $\theta_r$ . The "decrease in  $\theta_r$ " represents a 0.09 decrease from the base case to 0.01 for both Layers 1 and 2. The "increase in  $\theta_r$ " represents a 0.05 increase to 0.15 for both Layers 1 and 2. (b–d) Linear regression of the model predictions versus the field observations for the decrease (b) and increase (d) in  $\theta_r$ 

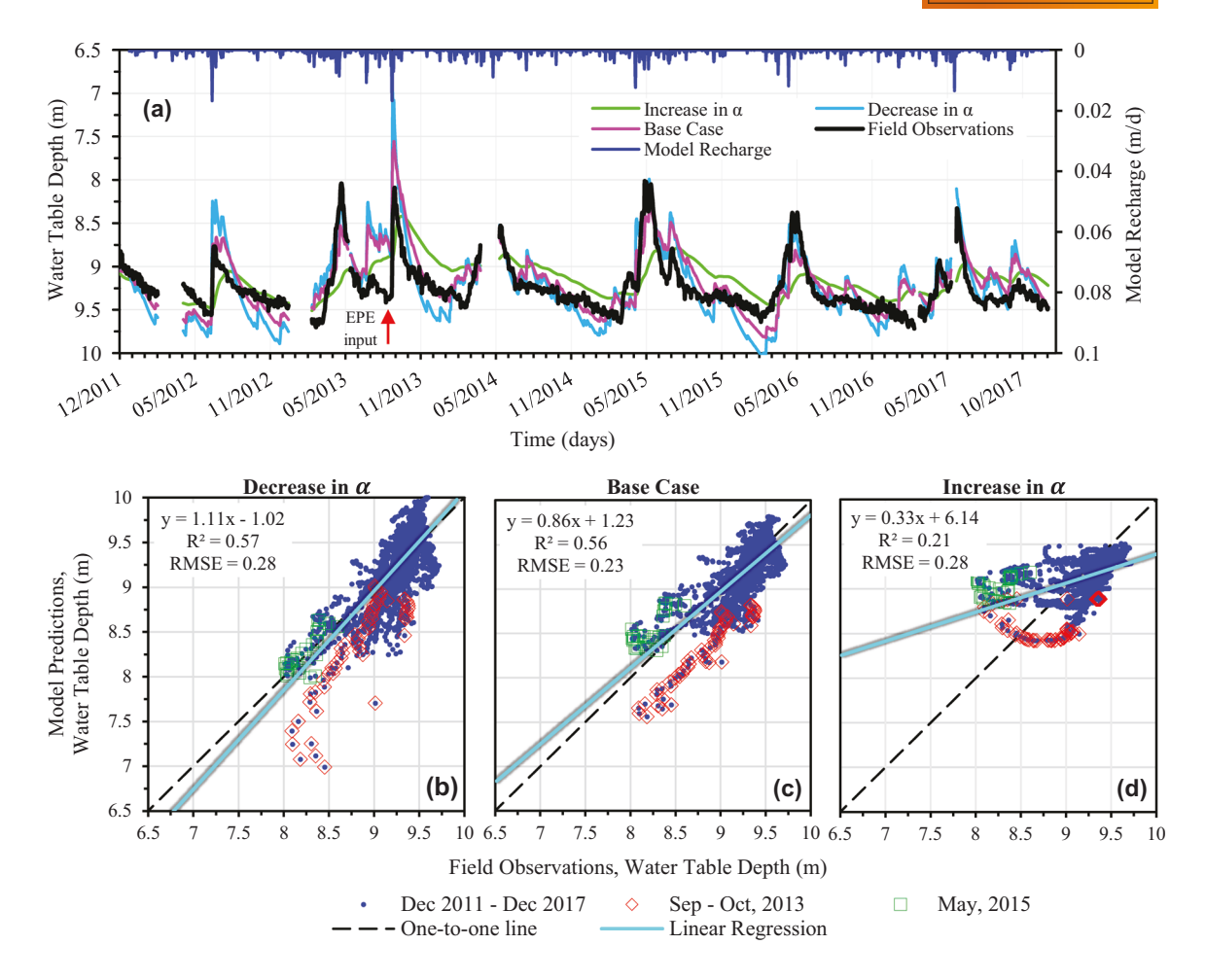
three van Genuchten parameters:  $\theta_r$ ,  $\alpha$ , and n for the soil layer and saprolite layer, respectively. For each model run, one of the three parameters is increased or decreased (Table 2).

Figure 4a shows model sensitivity to changes in residual water content,  $\theta_r$ . When  $\theta_r$  is decreased for both Layers 1 and 2, the modeled water table depth consistently predicts decreases in water table depths (overestimates). The decrease in  $\theta_r$  negatively affects the correlation between the field observed and base case, lowering the  $R^2$  to .45. The respective RMSE (0.24 m) indicates an acceptable model fit. Increasing  $\theta_r$  results in a dampened response where water table fluctuations are slightly subdued (Figure 4a,d). An increase in  $\theta_r$  results in a slightly exaggerated water table response. The  $R^2$  remains at .56, and the RMSE (0.30 m) indicates an acceptable model fit at the cusp of being a poor model fit.

Figure 5a shows model sensitivity to changes in  $\alpha$  (m<sup>-1</sup>), an empirical parameter that is inversely related to the airentry pressure value. The  $\alpha$  value chosen for the base case is  $\alpha = 0.18$  (m<sup>-1</sup>). For the sensitivity study,  $\alpha$  is initially

decreased for the soil and saprolite layers (Layers 1 and 2) to  $0.10~(\text{m}^{-1})$ . A decrease in  $\alpha$  allows the model to conform to field observations but consistently predicts slightly deeper water table depths (Figure 5a). Figure 5b shows that a decrease in  $\alpha$  slightly improves the  $R^2$  (.57). The respective RMSE (0.28 m) indicates an acceptable model fit. When  $\alpha$  values for are increased to 2.0, water table fluctuations are subdued (Figure 5a). The  $R^2$  value decreases (.21 m) with an increase in  $\alpha$ , suggesting a poor correlation (Figure 5d) between the model results and field observations. The respective RMSE (0.28 m) indicates an acceptable model fit.

Figure 6a shows the model sensitivity to changes in n (1), an empirical parameter that characterizes pore-size distribution. In HYDRUS-1D, n must be >1 (Equation 4). The default values for n are set by HYDRUS-1D and vary by soil type. For the base case, n = 1.50. For the sensitivity study, n is decreased to 1.25. A decrease in n allows the model to better conform to field observations but also consistently predicts slightly deeper water table depths (Figure 6a). The decrease



**FIGURE 5** (a) Time series of water table depths from field observations and model predictions (increase, base case, decrease) for alpha,  $\alpha$ . The "decrease in alpha,  $\alpha$ " represents a 0.08 decrease from the base case to 0.10 for both layers. The "increase in alpha,  $\alpha$ " represents a 1.82 increase to 2.00. (b–d) Linear regression of the model predictions versus the field observations for the decrease (b) and increase (d) in  $\alpha$ 

in n marginally improves (Figure 6b) the  $R^2$  (.58), and the RMSE (0.28 m) indicates an acceptable model fit. In contrast, an increase in n to 5.50 causes a dampened response, and water table fluctuations are subdued. An increase in n lowers  $R^2$  to .38 (Figure 6d), highlighting a poor correlation between field observations and model results. The respective RMSE (0.25 m) indicates an acceptable model fit.

# 3.3 | Soil water storage of the base case

In HYDRUS-1D, the soil water storage, V (m), is defined as the volume of water per unit area at a point in time. The V is calculated as:

$$V = \sum_{e} \Delta z_{i} \frac{\theta_{i} + \theta_{i+1}}{2} \tag{8}$$

where  $\theta_i$  and  $\theta_{i+1}$  are water contents evaluated at elements i and i+1, and  $\Delta z_i$  is the size of the element (Šimůnek et al., 2008, 2013). The summation in Equation 8 is taken over the

241 elements in the flow domain. Figure 7 shows the base case variability in soil water storage, *V*, from December 2011 to December 2017 by water year (WY). For example, WY2013 denotes the water year from 1 Oct. 2012 to 30 Sept. 2013. The dashed lines represent the average soil water storage for the respective water year.

The soil water storage, V, for the profile ranges from 6.50 to 6.62 m (Figure 7). The V values (e.g., 6.50 m) are the product of the average water content across the entire domain (e.g., 0.13) and the total column length (50 m;  $0.13 \times 50$  m = 6.50 m). As such, a higher V suggests that a greater portion of the available pore space is saturated, indicating that the subsurface is wetter than average (Figure 7). A lower V suggests that less of the available pore space is saturated, indicating that the subsurface is of average wet conditions or drier. A wetter subsurface may result in recharge, whereas a drier subsurface may result in little or no recharge. For example, V values from January 2013 and March 2013 show lower soil water storage, indicating little or no recharge. In contrast, after the September 2013 EPE, at the end of WY2013, the soil water storage is at its highest point in the

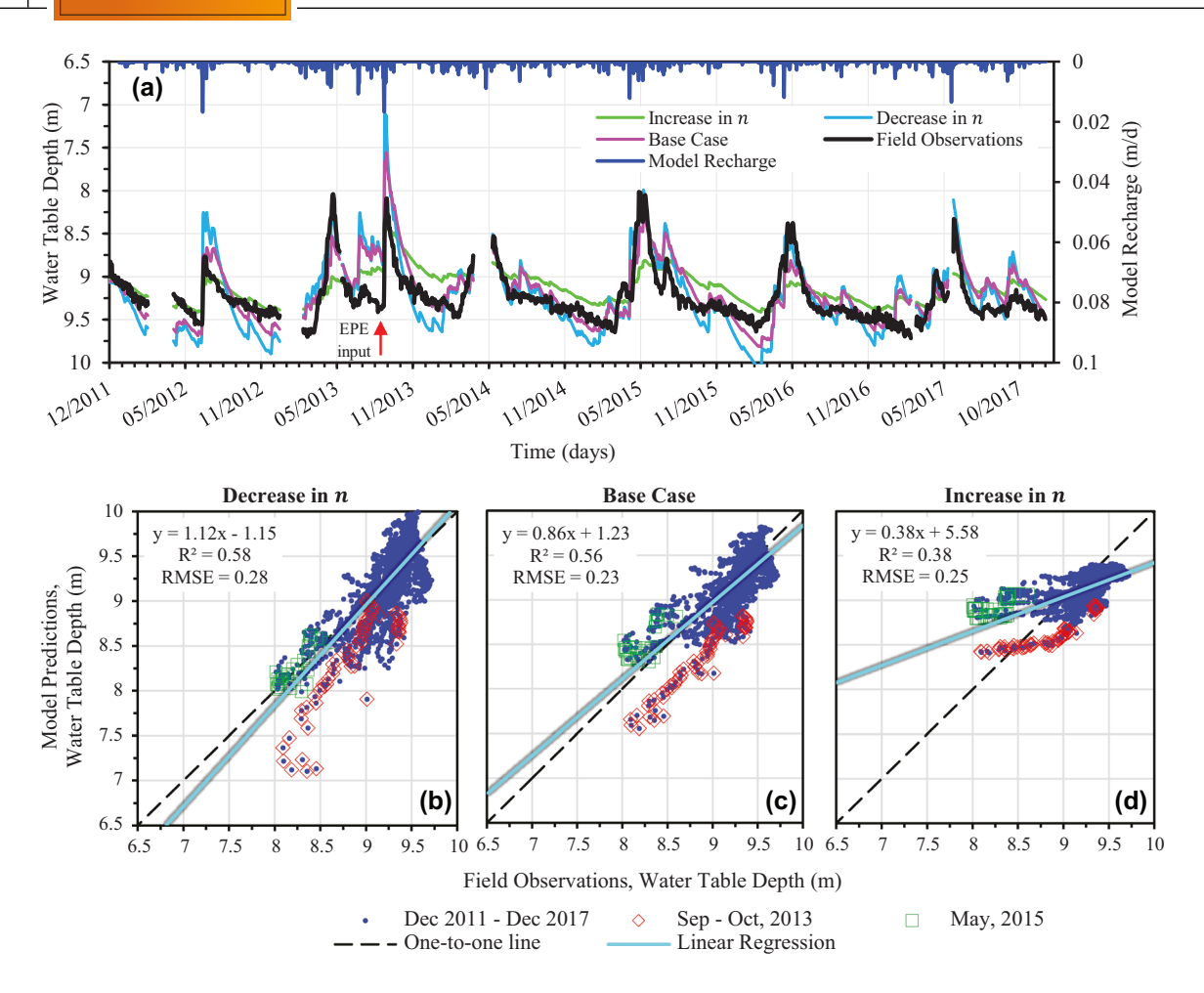


**FIGURE 6** (a) Time series of water table depths from field observations and model predictions (increase, base case, decrease) for the pore-size distribution, *n*. The "decrease in *n*" represents a 0.25 decrease from the base case to 1.25, for both layers. The "increase in *n*" represents a 4.00 increase to 5.50, for both layers (b–d). Linear regression of the model predictions versus the field observations for the decrease (b) and increase (d) in *n* 

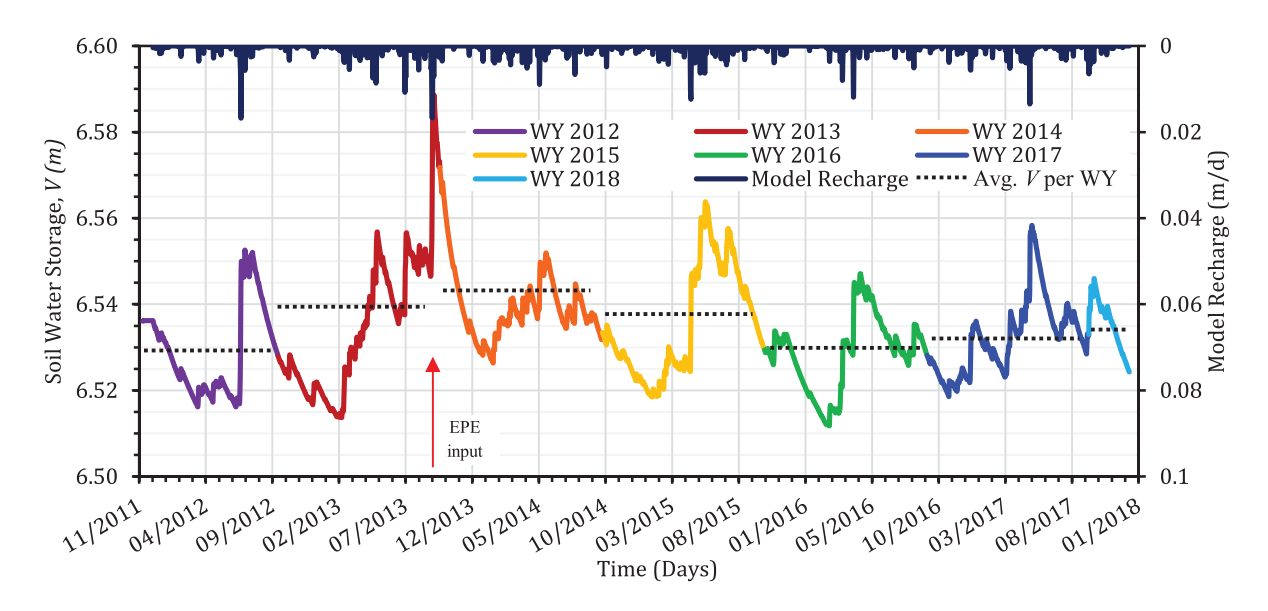


FIGURE 7 December 2011 to December 2017 time series of soil water storage, *V*, for the base case. The time series is split into water years (WY), a 12-mo period from 1 October to 30 September of the following year. The dotted lines denote average *V* per WY

6-yr record. The following WY2014 and WY2015 (dotted lines) exhibit the highest average *V* per water year, indicating that the EPE influenced subsurface processes for two water years after its occurrence.

## 4 | DISCUSSION

# 4.1 | How does the subsurface respond to the 2013 EPE in terms of water table fluctuations?

The September 2013 EPE had a long-term consequence in the subsurface, as shown by the Gordon Gulch field observations of water table fluctuations. The 1D, four-layered, homogeneous base case model represented the best scenario based on available data and provided model output that could most closely match the field observations. Visually, a comparison of the field observations and base case model showed good compatibility.

Figure 3a shows a consistent downward trend in the water table depth that reaches its deepest point (~9.6 m) every March of every year except 2014. In March 2014 (after the EPE), the deepest point is ~9.25 m, a shallower depth than every other year. It is not until March 2015 that the water table deepens to ~9.6 m again. We speculate that the contrast between the consistent water table depths of ~9.6 m and the shallower water table depth of March 2014 (~9.2 m) provide evidence that the water table remained shallower in large part due to the EPE footprint, which remained until at least March 2015. The field observations and model results agree that the subsurface continued to respond to the EPE infiltration flux for at least 18 mo after the event, which is longer than previously suggested (Henning, 2016).

For further comparison between the field observations and model results, we calculated the  $R^2$  to measure the goodness of fit between the field observations and base case model. In addition, the RMSE was used to calculate the square root of the variance of the residuals to indicate how close the observed data are to the model results. The base case model is considered an acceptable model fit, as indicated by the  $R^2$ (.56) coefficient and the RMSE (0.23 m) value (Table 3). The results present opportunities for improvements while highlighting the limitations of the 1D modeling approach. For example, the 1D modeling approach does not simulate lateral flow process at the hillslope scale or regional scale, which could affect the goodness of fit. The greatest deviation in correlation occurred during the EPE, where the base case predicted a higher water table (~7.5 m) than the field observations (~8.2 m), though this value was still within a 10% margin of the field data. Although out of the scope of this study, a two-dimensional or three-dimensional model accounting for lateral flow may improve the goodness of fit between the field observations and modeled results.

# **4.2** | Sensitivity analysis of hydraulic parameters

A sensitivity analysis examined how model response may be affected by parameter change. The  $R^2$  value calculated for each sensitivity analysis ranged from .21 (poor correlation) to .58 (acceptable correlation). The RMSE value calculated for each sensitivity analysis ranged from 0.24 to 0.30 m (Table 3). All RMSE values were indicative of acceptable model fit, with one model (increase in  $\theta_r$ ) at the cusp between acceptable and poor, despite an acceptable  $R^2$  value. The lack of RMSE values indicating a good fit model could be attributable to the high sensitivity that the RMSE has to outliers (i.e., the largest differences between field observations and model results). Two EPEs of different temporal extents—the September 2013 EPE and the May 2015 month-long rain event—resulted in large differences between the field observations of water table depths and the model results. These EPE-derived outliers skewed the RMSE away from indicating a good model fit. Future studies examining EPEs may benefit from statistical methods that are not strongly biased toward outliers.

The visual outcome of the sensitivity runs can be described by two general responses: dampened or exaggerated (Table 3). An exaggerated response indicates shallower and deeper water table depths relative to the base case. A dampened response would indicate the opposite of exaggeration (i.e., more smoothed, tempered variation).

#### 4.2.1 | Residual water content

From the sensitivity analysis, decreasing the residual water content,  $\theta_r$  (Figure 4d), yields a dampened water table response. Increasing the  $\theta_r$  (Figure 4b) yields an exaggerated water table response. These responses are likely due to the local effective porosity of the material (Horton et al., 1988). The effective porosity, also thought of as the "drainable porosity," is defined as the percentage of interconnected void space with respect to the bulk volume (Brooks & Corey, 1964).

$$\phi = \frac{V_{\rm p}}{V_{\rm b}} \tag{9}$$

where  $\varphi$  is the effective porosity (1),  $V_p$  is the total volume of interconnected voids (m³), and  $V_b$  is the bulk volume (m³). A soil with a higher  $\varphi$  has a larger total volume of  $V_p$  relative to  $V_b$ . Decreasing  $\theta_r$  (with  $\theta_s$  held constant) increases the total volume of  $V_p$  relative to  $V_b$ , indicating a higher  $\varphi$ . Decreasing  $\theta_r$  can result in water being more readily held in pore spaces (higher  $\varphi$ ), slowing the rate of flow. Water held in pore spaces may result in a slower drainage out of the pore spaces, which can dampen fluctuations of the water table. In contrast, increasing  $\theta_r$  (with  $\theta_s$  held constant) decreases the

TABLE 3 Model response to increases and decreases of the van Genuchten parameters

Parameters	Residual water content	Parameter inversely related to the air-entry pressure	Pore-size distribution	Base case
		$m^{-1}$		
Parameter change	Increase	Increase	Increase	$R^2 = .56,$
Water table response	Exaggerated	Dampened	Dampened	RMSE = 0.23
$R^2$ value	.56	.21	.38	
RMSE	0.30	0.28	0.25	
Parameter change	Decrease	Decrease	Decrease	
Water table response	Dampened	Exaggerated	Exaggerated	
$R^2$ value	.45	.57	.58	
RMSE	0.24	0.28	0.28	

total volume of  $V_{\rm p}$  relative to  $V_{\rm b}$ , indicating a lower  $\varphi$ . A lower  $\varphi$  can be indicative of a faster draining soil with minimal available pore space for water to fill. A low  $\varphi$  may allow faster flow through the subsurface, thus resulting in more rapid water table response (Figure 4b).

# 4.2.2 | Air-entry pressure

The alpha parameter,  $\alpha$  (m<sup>-1</sup>), is inversely related to the air-entry pressure, the matric suction value required to fill (empty) pore spaces (Nimmo, 2004). Its purpose is to serve as an approximation of the steepest section of the soil water retention curve (van Genuchten, 1980). Where the soil water retention curve is steepest, the water content (typically plotted on the y-axis) is most sensitive to changes in the pressure head (typically plotted on the x-axis). This is also mathematically evident in the van Genuchten equations (Equation 2), where  $\alpha$  as part of the denominator influences the fraction from which the quotient determines water content as a function of pressure head,  $\theta(\psi)$  given  $\psi < 0$  (Brooks & Corey, 1964; Mualem, 1976; van Genuchten, 1980). The base case  $\alpha = 0.18$  m<sup>-1</sup> is considered the best fit for the field data.

Results from the sensitivity study show that decreasing  $\alpha$  (relative to the base case) causes the water table to fluctuate more rapidly (Figure 5a). Conceptually, a decrease in  $\alpha$  translates to an increase (due to the inverse relation) in the minimum matric suction value that air must attain to enter a pore space. While pressure builds so that air can attain the higher matric suction to enter a pore space, water can enter (drain from) these same pores with greater ease. The ease at which water can fill (drain) pores in the unsaturated zone is known as the unsaturated hydraulic conductivity, K (m d<sup>-1</sup>). A decrease in  $\alpha$  can allow water to fill (empty) pores with greater ease, resulting in a larger K value, which consequently results in more rapid downward flow, and thus more dramatic water table fluctuations, as seen in Figure 5a.

An increase in  $\alpha$  translates to a decrease (due to the inverse relation) in the minimum matric suction value that air must attain to enter a pore space. A lower minimum matric suction value means that air can more easily enter (exit) pores. Water has difficulty entering pore spaces now relative to air, and as a result the unsaturated hydraulic conductivity, K of the soil decreases. A smaller K value implies slower and delayed downward flow to the water table. The downward flow is dampened with time as it slowly moves downward, resulting in smoother water table fluctuations (Figure 5a).

# 4.2.3 | Pore-size distribution

Changes to the pore-size distribution parameter, n, result in higher correlation between the field observations and model results. In the van Genuchten soil hydraulic functions used to determine  $\theta$  (Equation 2), both  $\alpha$  and  $\psi$  are raised to the power of n. The n parameter is further used to determine the empirical parameter, m (1) (Equation 4), where m is an exponent used to solve for the unsaturated hydraulic conductivity and the soil water retention (Equations 2 and 3). Figure 6 shows that a decrease in n causes an exaggerated response, whereas an increase in n causes a dampened response. Physically, nrepresents the allowed abundance of varying pore sizes in a volume of soil (Nimmo, 2004). When water infiltrates a soil with a narrow and uniform distribution of pore sizes, the water flux can more easily fill (or empty) pores at the same matric suction. In the subsurface, matric suction is defined as the difference between pore air pressure and pore water pressure. Conventionally, pore air pressure is equal to atmospheric pressure and is ignored (Chiorean, 2017).

Expanding the allowed distribution of pore sizes (higher *n*) increases the possible variation of pore sizes. A soil with more highly varying pore sizes requires highly varying matric suction for water to fill (empty) the varying size pores, generally retarding downward flow (Nimmo, 2004; Zhang et al., 2019).

In response, the water flux becomes dampened in the subsurface, visually translating to a smoother water table response (Figure 6). In contrast, narrowing the allowed distribution of pore sizes (smaller *n*) reduces the possible variation of pore sizes. Reducing the possible variations in pore sizes allows water to fill (empty) pores more easily with the same matric suction. Such ease allows water to flow downward at a faster rate, resulting in a more exaggerated water table response (Figure 6a).

# 4.3 | How does soil water storage respond to the EPE?

The modeled changes in soil water storage suggest new developments that affect our understanding of how the subsurface responded to the 2013 EPE. First, there was a rapid increase in soil water storage in late WY2013. After the EPE, soil water storage remained elevated through WY2014 and into WY2015. The early part of WY2014 had comparatively higher soil water storage during the winter months (December 2013–March 2014) relative to all other water years for the same time frame. The heightened soil water storage during this time frame may be a strong indicator that recharge occurred for several months after the EPE, especially because minimal evapotranspiration occurs in the area during the winter season.

The increase in *V* (Figure 7, dotted lines) post-EPE is sustained through WY2015. During WY2016 (February 2016), the soil water storage once again reaches a winter low as seen during WY2012 (February 2012) and WY2013 (February 2013), pre-EPE. The modeled changes in soil water storage suggest that a 2-yr recovery occurred in response to the EPE-induced infiltration flux.

#### 5 | CONCLUSIONS

The 2013 Colorado EPE not only flooded the surface and rivers downstream but resulted in rapid infiltration and heightened water table response. Here are the conclusions we draw from this study:

- 1. Both the field observations and model results showed a water table rise after the EPE, which persisted for  $\sim$ 18 mo before the water table recovered to pre-EPE levels.
- 2. Average annual soil water storage post-EPE for WY2014 and WY2015 was higher than all other water years in the record, indicating a wetter subsurface post-EPE.
- 3. The post-EPE could serve as a hydrologic buffer that stores a portion of extreme precipitation for various seasons.
- 4. A sensitivity study of model parameters showed that the modeled water table was most sensitive to changes in the

empirical parameter that represents the pore size distribution value, n. Pore-size distribution cannot be measured in the field, it is essential to scrutinize the values to which empirical parameters are set in simulations.

Given the characteristics in geology, hydrology, and geographic considered herein, the model setup and results could be applicable to regions of similar characteristics. By assessing the potential for unsaturated zone profiles to serve as natural storage space for EPE-induced infiltration, this study could provide a scientific basis for water managers to timely use the stored water that may be released to streams over time. More research regarding local subsurface response to EPEs is needed because EPEs are predicted to occur more frequently worldwide (Lehmann et al., 2015; Trenberth, 2011; Wasko et al., 2016). Understanding the effects of individual EPEs on the subsurface could also provide the basis for predicting aggregated effects over longer time scales. From another viewpoint, in headwater regions, snowmelt is the primary source of groundwater recharge. Although the rate of snowmelt is typically not as dramatic as EPEs, snow could occur at an accelerated rate under warming (Pepin et al., 2015). This study could be informative for projecting the potential hydrologic consequences of accelerated snowmelt. More broadly, the results of this study contribute to a better understanding of how the subsurface can act as a long-term hydrologic buffer for infiltration from an EPE before recharge occurs.

### **ACKNOWLEDGMENTS**

This research was supported by the National Science Foundation, Division of Earth Sciences EAR (Grant 1834290). The authors appreciate the constructive comments from three anonymous reviewers and the associate editors.

#### AUTHOR CONTRIBUTIONS

Claudia R. Corona: Conceptualization; Data curation; Formal analysis; Investigation; Methodology; Validation; Visualization; Writing – original draft; Writing – review & editing. Shemin Ge: Conceptualization; Funding acquisition; Project administration; Resources; Supervision; Writing – review & editing.

#### CONFLICT OF INTEREST

The authors declare no conflict of interest.

### ORCID

Claudia R. Corona https://orcid.org/0000-0002-6447-9175

### REFERENCES

Anderson, S., & Ragar, D. (2021a). BCCZO—Well water levels—(GGU\_GW\_1,2,6\_Pducer\_Tran)—Gordon Gulch: Upper—(2011–2020).

- **Hydroshare**. https://www.hydroshare.org/resource/4a4b2b04790147-828072151b2a4820e1/
- Anderson, S., & Ragar, D. (2021b). BCCZO Streamflow/Discharge (GGL\_SW\_0\_Dis) Gordon Gulch: Lower (2011-2019). HydroShare. http://www.hydroshare.org/resource/c2384bd1743a42-76a88a5110b1964ce0
- Anderson, S. P., Anderson, R. S., Tucker, G. E., & Dethier, D. P. (2013).
  Critical zone evolution: Climate and exhumation in the Colorado Front Range. In L. D. Abbott & G. S. Hancock (Eds.), Classic concepts and new directions: Exploring 125 years of GSA discoveries in the rocky mountain region. Geological Society of America. <a href="https://doi.org/10.1130/2013.0033(01">https://doi.org/10.1130/2013.0033(01)</a>
- Boulder Area Sustainability Information Network (BASIN). (2005). 1894 flood of Boulder Creek. http://bcn.boulder.co.us/basin/history/1894flood.html
- Boulder Creek Critical Zone Observatory (BcCZO). (2020). Gordon Gulch. https://czo-archive.criticalzone.org/boulder/infrastructure/field-area/gordon-gulch/#settingResearch
- Befus, K. M., Sheehan, A. F., Leopold, M., Anderson, S. P., & Anderson, R. S. (2011). Seismic constraints on critical zone architecture, Boulder Creek Watershed, Front Range, Colorado. *Vadose Zone Journal*, 10(3), 915–927. https://doi.org/10.2136/vzj2010.0108
- Brooks, R. H., & Corey, A. T. (1964). Hydraulic properties of porous media. Hydrology Papers Colorado State University, 3, 37.
- Chiorean, V.-F. (2017). Determination of matric suction and saturation degree for unsaturated soils, comparative study: Numerical method versus analytical method. *IOP Conference Series: Materials Science* and Engineering, 245, 032074. https://doi.org/10.1088/1757-899X/ 245/3/032074
- Coffman, K. (2013). Property losses from Colorado flood projected at about \$2 billion. Reuters. https://www.reuters.com/article/us-usacolorado-flooding/property-losses-from-colorado-flood-projectedat-about-2-billion-idUSBRE98H1BA20130919
- Corona, C. R., Gurdak, J. J., Dickinson, J. E., Ferré, T. P. A., & Maurer, E. P. (2018). Climate variability and vadose zone controls on damping of transient recharge. *Journal of Hydrology*, 561, 1094–1104. https://doi.org/10.1016/j.jhydrol.2017.08.028
- Dadgar, M. A., Nakhaei, M., Porhemmat, J., Eliasi, B., & Biswas, A. (2020). Potential groundwater recharge from deep drainage of irrigation water. *Science of The Total Environment*, 716, 137105. https://doi.org/10.1016/j.scitotenv.2020.137105
- Freeze, R. A., & Witherspoon, P. A. (1967). Theoretical analysis of regional groundwater flow: 2. Effect of water-table configuration and subsurface permeability variation. *Water Resources Research*, *3*(2), 623–634. https://doi.org/10.1029/WR003i002p00623
- French, R. H., Jacobson, R. L., & Lyles, B. F. (1996). Threshold precipitation events and potential ground-water recharge. *Journal of Hydraulic Engineering*, 122(10), 573–578. https://doi.org/10.1061/(ASCE)0733-9429(1996)122:10(573)
- Van Genuchten, M. T.h. (1980). A closed-form equation for predicting the hydraulic conductivity of unsaturated soils. *Soil Science Society of America Journal*, 44(5), 892–898. https://doi.org/10.2136/sssaj1980. 03615995004400050002x
- Gurdak, J. J., Hanson, R. T., & Green, T. R. (2009). Effects of climate variability and change on groundwater resources of the United States (Fact Sheet No. 2009–3074). USGS.
- Hale, K. E., Wlostowski, A. N., Badger, A. M., Musselman, K. N., Livneh, B., & Molotch, N. P. (2022). Modeling streamflow sensitivity to climate warming and surface water inputs in a montane

- catchment. *Journal of Hydrology: Regional Studies*, *39*, 100976. https://doi.org/10.1016/j.ejrh.2021.100976
- Henning, S. (2016). *Dynamic response of watershed sub-surface systems to extreme precipitation events* [Master's thesis, University of Colorado]. https://www.proquest.com/openview/cde11384a660bce26521062eea8c5f70/1?pq-origsite=gscholar&cbl=18750
- Hopmans, J. W., & Stricker, J. N. M. (1989). Stochastic analysis of soil water regime in a watershed. *Journal of Hydrology*, 105, 57–84. https://doi.org/10.1016/0022-1694(89)90096-6
- Horton, R., Thompson, M. L., & McBride, J. F. (1988). Determination of effective porosity of soil materials. USEPA.
- Jasechko, S., & Taylor, R. G. (2015). Intensive rainfall recharges tropical groundwaters. *Environmental Research Letters*, 10(12), 124015. https://doi.org/10.1088/1748-9326/10/12/124015
- Kløve, B., Ala-Aho, P., Bertrand, G., Gurdak, J. J., Kupfersberger, H., Kværner, J., Muotka, T., Mykrä, H., Preda, E., Rossi, P., Uvo, C. B., Velasco, E., & Pulido-Velazquez, M. (2013). Climate change impacts on groundwater and dependent ecosystems. *Journal of Hydrology*, 518, 250–266. https://doi.org/10.1016/j.jhydrol.2013.06.037
- Langston, A. L., Tucker, G. E., Anderson, R. S., & Anderson, S. P. (2015). Evidence for climatic and hillslope-aspect controls on vadose zone hydrology and implications for saprolite weathering: Climatic control on vadose zone moisture. *Earth Surface Processes and Landforms*, 40(9), 1254–1269. https://doi.org/10.1002/esp.3718
- Lehmann, J., Coumou, D., & Frieler, K. (2015). Increased record-breaking precipitation events under global warming. *Climatic Change*, 132(4), 501–515. https://doi.org/10.1007/s10584-015-1434-y
- Mo'allim, A., Kamal, M., Muhammed, H., Yahaya, N., Zawawe, M., Man, H., & Wayayok, A. (2018). An assessment of the vertical movement of water in a flooded paddy rice field experiment using Hydrus-1D. *Water*, 10(6), 783. https://doi.org/10.3390/w10060783
- Moriasi D. N., Arnold J. G., Van Liew M. W., Bingner R. L., Harmel R. D., & Veith T. L., (2007). model evaluation guidelines for systematic quantification of accuracy in watershed simulations. *Transactions of the ASABE*, 50(3), 885–900. https://doi.org/10.13031/2013.23153
- Mualem, Y. (1976). A new model for predicting the hydraulic conductivity of unsaturated porous media. *Water Resources Research*, *12*(3), 513–522. https://doi.org/10.1029/WR012i003p00513
- National Atmospheric Deposition Program (NADP). (2020). Site NTN CO94. https://nadp.slh.wisc.edu/sites/ntn-co94/
- Neto, D. C., Chang, H. K., & van Genuchten, M. T. (2016). A mathematical view of water table fluctuations in a shallow acquifer in Brazil. *Groundwater*, 54(1), 82–91. https://doi.org/10.1111/gwat.12329
- Ng, G. H. C., McLaughlin, D., Entekhabi, D., & Scanlon, B. R. (2010).
  Probabilistic analysis of the effects of climate change on groundwater recharge. Water Resources Research, 46(7), W07502. https://doi.org/10.1029/2009WR007904
- Nimmo, J. R. (2004). Porosity and pore size distribution. In D. Hillel & J. L. Hatfield (Eds.), *Encyclopedia of soils in the environment* (vol. 3, pp. 295–303). USGS.
- Nimmo, J. R. (2006). Unsaturated zone flow processes. In M. G. Anderson & J. J. McDonnell (Eds.), *Encyclopedia of hydrological sciences*. John Wiley and Sons. http://doi.wiley.com/10.1002/0470848944.hsa161
- Pendergrass, A. G., & Knutti, R. (2018). The uneven nature of daily precipitation and its change. *Geophysical Research Letters*, 45(21), 11,980–11,988. https://doi.org/10.1029/2018GL080298

- Pepin, N., Bradley, R. S., Diaz, H. F., Baraër, M., Caceres, E. B., Forsythe, N., Fowler, H. J., Greenwood, G., Zia ur Rahman Hashmi, M., Liu, X. D., Miller, J. R., Ning, L., Ohmura, A., Palazzi, E., Rangwala, I., Schöner, W., Severskiy, I., Shahgedanova, M., Wang, M. B., Williamson, S, N., & Yang, D. (2015). Elevation-dependent warming in mountain regions of the world. *Nature Climate Change*, 5(5), 424–430. https://doi.org/10.1038/nclimate2563
- Pfahl, S., O'Gorman, P. A., & Fischer, E. M. (2017). Understanding the regional pattern of projected future changes in extreme precipitation. *Nature Climate Change*, 7(6), 423–427. https://doi.org/10.1038/ nclimate3287
- Prein, A. F., Rasmussen, R. M., Ikeda, K., Liu, C., Clark, M. P., & Holland, G. J. (2017). The future intensification of hourly precipitation extremes. *Nature Climate Change*, 7(1), 48–52. https://doi.org/10.1038/nclimate3168
- Reitz, M., Sanford, W. E., Senay, G. B., & Cazenas, J. (2017). Annual estimates of recharge, quick-flow runoff, and evapotranspiration for the contiguous US using empirical regression equations. *Journal of the American Water Resources Association*, 53(4), 961–983. https://doi.org/10.1111/1752-1688.12546
- Reusser, D. E., Blume, T., Schaefli, B., & Zehe, E. (2009). Analysing the temporal dynamics of model performance for hydrological models. *Hydrology and Earth System Sciences*, 13(7), 999–1018.
- Richards, L. A. (1931). Capillary conduction of liquids through porous mediums. *Physics*, 1(5), 318–333. https://doi.org/10.1063/1.1745010
- Salberg, L. (2021). Coupling field data and a flow model to characterize the role of groundwater in a montane, semi-arid, headwater catchment, Gordon Gulch, Colorado [Master's thesis, University of Colorado]. https://www.proquest.com/openview/292ac52a5775fd6156b5172263db58f9/1.pdf?pq-origsite=gscholar&cbl=18750&diss=y
- Sanford, W. E., & Selnick, D. L. (2013). Estimation of evapotranspiration across the conterminous United States using a regression with climate and land-cover data. *Journal of the American Water Resources Association*, 49(1), 217–230. https://doi.org/10.1111/jawr.12010
- Schaap, M. G., & Leij, F. J. (2000). Improved prediction of unsaturated hydraulic conductivity with the Mualem-van Genuchten model. *Soil Science Society of America Journal*, 64(3), 843–851. https://doi.org/ 10.2136/sssaj2000.643843x
- Schaap, M. G., Leij, F. J., & Van Genuchten, M. Th. (2001). Rosetta: A computer program for estimating soil hydraulic parameters with hierarchical pedotransfer functions. *Journal of Hydrology*, 251(3–4), 163–176. https://doi.org/10.1016/S0022-1694(01)00466-8
- Shao, J., Si, B., & Jin, J. (2018). Extreme precipitation years and their occurrence frequency regulate long-term groundwater recharge and transit time. *Vadose Zone Journal*, 17(1), 1–9. https://doi.org/10. 2136/vzj2018.04.0093
- Shea, N. (2013). Spatial patterns of mobile regolith thickness and meteoric 10Be in Gordon Gulch, Front Range, CO [Master's thesis, University of Connecticut]. https://opencommons.uconn.edu/gs\_theses/ 463
- Šimůnek, J., Genuchten, M. T. H., & Šejna, M. (2008). Development and applications of the HYDRUS and STANMOD software packages and related codes. *Vadose Zone Journal*, 7(2), 587–600. https://doi.org/10.2136/vzj2007.0077
- Šimůnek, J., Sejna, M., Saito, H., Sakai, M., & van Genuchten, M. T. (2013). The HYDRUS-1D software package for simulating the one-dimensional movement of water, hear, and multiple solutes in

- variably-saturated media. Department of Environmental Sciences, University of California Riverside.
- Singh, J., Knapp, H. V., & Demissie, M. (2005). Hydrologic modeling of the Iroquois River watershed using HSPF and SWAT. *Journal of the American Water Resources Association*, *41*(2), 343–360. https://doi.org/10.1111/j.1752-1688.2005.tb03740.x
- Tashie, A. M., Mirus, B. B., & Pavelsky, T. M. (2016). Identifying long-term empirical relationships between storm characteristics and episodic groundwater recharge. *Water Resources Research*, 52(1), 21– 35. https://doi.org/10.1002/2015WR017876
- Thomas, B., Behrangi, A., & Famiglietti, J. (2016). Precipitation intensity effects on groundwater recharge in the southwestern United States. *Water*, 8(3), 90. https://doi.org/10.3390/w8030090
- Trenberth, K. E. (2011). Changes in precipitation with climate change. Climate Research, 47(1), 123–138. https://doi.org/10.3354/cr00953
- Trenberth, K. E., Dai, A., Rasmussen, R. M., & Parsons, D. B. (2003).
  The changing character of precipitation. *Bulletin of the American Meteorological Society*, 84(9), 1205–1218. https://doi.org/10.1175/BAMS-84-9-1205
- Uccellini, L. (2014). The record Front Range and eastern Colorado floods of September 11 - 17, 2013 (National Weather Service, National Oceanic and Atmospheric Administration. https://repository.library. noaa.gov/view/noaa/6979
- Vanapalli, S. K., Sillers, W. S., & Fredlund, M. D. (1998). *The meaning and relevance of residual state to unsaturated soils*. 51st Canadian Geotechnical Conference, Edmonton, AB, Canada. http://by.genie.uottawa.ca/~vanapall/papers/conference/1998/cgs98\_residual.pdf
- Vereecken, H., Huisman, J. A., Hendricks Franssen, H. J., Brüggemann, N., Bogena, H. R., Kollet, S., Javaux, M., Van Der Kruk, J., & Vanderborght, J. (2015). Soil hydrology: Recent methodological advances, challenges, and perspectives: Soil hydrology. Water Resources Research, 51(4), 2616–2633. https://doi.org/10.1002/ 2014WR016852
- Vogel, T., Van Genuchten, M. T.h., & Cislerova, M. (2001). Effect of the shape of the soil hydraulic functions near saturation on variablysaturated flow predictions. Advances in Water Resources, 24(2), 133– 144.
- Wasko, C., Sharma, A., & Westra, S. (2016). Reduced spatial extent of extreme storms at higher temperatures. *Geophysical Research Letters*, 43(8), 4026–4032. https://doi.org/10.1002/2016GL068509
- Westra, S., Alexander, L. V., & Zwiers, F. W. (2013). Global increasing trends in annual maximum daily precipitation. *Journal of Climate*, 26(11), 3904–3918. https://doi.org/10.1175/JCLI-D-12-00502.1
- Yates, S. R., Van Genuchten, M. T.h., Warrick, A. W., & Leij, F. J. (1992). Analysis of measured, predicted, and estimated hydraulic conductivity using the RETC computer program. *Soil Science Society of America Journal*, 56, 347–354. https://doi.org/10.2136/sssaj1992.03615995005600020003x
- Zhang, C., & Lu, N. (2019). Unitary definition of matric suction. *Journal of Geotechnical and Geoenvironmental Engineering*, 145(2), 1. https://doi.org/10.1061/(ASCE)GT.1943-5606.0002004

**How to cite this article:** Corona, C. R., & Ge, S. (2022). Examining subsurface response to an extreme precipitation event using HYDRUS-1D. *Vadose Zone Journal*, e20189. https://doi.org/10.1002/vzj2.20189